

Instrument Science Report WFC3 2010-14

## The Photometric Performance of WFC3/UVIS: Temporal Stability Through Year 1

J. S. Kalirai, S. Baggett, T. Borders, and A. Rajan

October 14, 2010

---

### ABSTRACT

*We analyze multiple observations of three bright HST spectrophotometric standard stars obtained with WFC3 UVIS1 and UVIS2 in order to establish the temporal stability of the instrument over its first year of science operations. Observations of the three stars, GD 153, G191B2B, and GRW+70d5824 were obtained at multiple dither positions at each epoch and in most Wide (W) and Medium (M) band filters. The cadence of the observations was varied from once per week shortly after the instrument was installed in Hubble in the summer of 2009 (i.e., during SMOV) to once ever few months toward the end of the first year. Analysis of the high signal-to-noise photometry in W and M bands indicates that the instrument is photometrically stable, with measured variations that are  $<0.4\%$ .*

---

### 1. Monitoring Observations During WFC3's First Year

A primary advantage of the Hubble Space Telescope (HST) over ground based facilities is that it is very stable. Except for passing in and out of earth shadow, the environment is constant, and except for occasional instrument replacements, the configuration of the telescope is fixed. As a result, Hubble's instruments can provide unprecedented characterization of transient phenomena that vary over periods ranging from a few minutes to several years. Our ability to accurately characterize such sources requires knowledge of the end-to-end telescope/instrument spatial and temporal stability. The spatial stability can be characterized by low frequency flat field variations, as constrained through observations of dense fields (e.g., see Sabbi 2009). For the temporal stability, the best strategy is to monitor bright and isolated sources with very high signal-to-noise observations over a sufficient baseline.

Since its installation in Hubble in May 2009, the WFC3 instrument has quickly emerged as a powerful and unique tool for astrophysical investigations. During this time, several WFC3 calibration programs have been executed to establish the instrument’s performance in orbit, the results of which are summarized in dozens of ISRs (available at <http://www.stsci.edu/hst/wfc3/documents/ISRs/>). Several of the larger programs in this extensive (SMOV and Cycle 17) calibration effort have primary goals of measuring WFC3’s absolute sensitivity through standard star observations, as well as the measurement of possible contamination in the UV filters. By design, these programs image point sources with a specific cadence and in a specific instrumental setup, and therefore the data can be analyzed to put the first constraints on the temporal stability of WFC3.

## 2. The Data Set

The observations that we analyze in this ISR come from 1.) SMOV Proposal CAL11426 – *UVIS SMOV Contamination Monitor*, 2.) Cycle 17 Proposal CAL11907 – *UVIS Cycle 17 Contamination Monitor*, 3.) SMOV Proposal CAL11450 – *UVIS Photometric Zero Points*, and 4.) Cycle 17 Proposal CAL11903 – *UVIS Photometric Zero Points*. The first and second programs imaged the hot white dwarf GRW+70d5824, on both CCDs, with a cadence of once per week during SMOV and once every 2-4 weeks during Cycle 17. The observations were taken using 9 WFC3 UV filters on most visits, as well as F606W and F814W. The third program obtained observations of the bright spectrophotometric standard GD 153 in 37 UVIS filters initially, as well as repeat observations in 8 wide band filters at a cadence of 1 day, 1 week, and 1 month during SMOV (i.e., July – August 2009). The second program was the more ambitious Cycle 17 version, where a standard star was observed in all 62 UVIS filters on both CCDs including repeat observations in W and M bands for multiple standards. For our present purposes, we analyze the full data sets from CAL11426 and CAL11907 and a subset of the data set of 11450 and 11903 that includes repeat observations of the HST standards G191B2B and GD 153 in Wide (W) and Medium (M) band filters. The time baseline of these observations extends from the end of SMOV to August 2010.

We summarize the imaging data of each of these three stars, the filters they were observed with, as well as the cadence of the observations in Table 1.

## 3. Photometry Analysis

The data were retrieved from the Multimission Archive at Space Telescope (MAST) and processed with the IRAF/STSDAS pipeline program calwf3. Earlier data sets obtained during SMOV and reported in Kalirai et al. (2009) were all reprocessed with the updated calwf3 pipeline (version 2.0) and a common set of calibration files. At the time these data were processed, the pipeline still used a ground-based flat field and preliminary geometric distortion solution. Although these calibration products are important for an absolute measurement of WFC3’s throughput, our present analysis is not affected since we are solely interested in a relative measurement where the star is at the same location on the detector in each epoch.

Table 1: WFC3 UVIS1 and UVIS2 Temporal Stability Observations

Target	Detector	Filters	Cadence (days)
GD 153	UVIS1	F225W, F275W, F336W F390W, F438W, F555W	1, 2, 9, 29, 126, 145, 204, 264, 318
GD 153	UVIS1	F475W	1, 126, 145, 204, 264, 318
GD 153	UVIS1	F606W, F814W	1, 2, 9, 29, 204
GD 153	UVIS2	F606W, F814W, F467M F547M, F469N, F502N	1, 19, 138, 192
G191B2B	UVIS1	F225W, F275W, F336W, F350LP F390W, F438W, F475W, F555W	1, 10, 43, 68, 158
G191B2B	UVIS1	F850LP	1, 43, 68, 158
G191B2B	UVIS2	F606W, F814W, F467M F547M, F469N, F502N	1, 10, 43, 68, 158
GRW+70d5824	UVIS1	F218W, F225W, F275W, F336W F390M, F390W, F438W, F475W F547M, F606W, F814W	1 – 418 (up to 40 epochs)
GRW+70d5824	UVIS2	F218W, F225W, F275W, F336W F390M, F390W, F438W, F475W F547M, F606W, F814W	1 – 414 (up to 20 epochs)

All of the observations presented in this ISR were obtained using a 512 pixel subarray to minimize readout times. These subarrays are located in the corners of the WFC3 4k x 4k mosaic, regions of the detector where constraints on the flat field are worst and also where the geometric distortion correction is largest (both effects will impact absolute throughput measurements). The two subarrays used on UVIS1 are UVIS1-C512A-SUB and UVIS1-C512B-SUB and the two subarrays on UVIS2 are UVIS2-C512C-SUB and UVIS2-C512D-SUB, as illustrated in Figure 1. With this subarray size, radial apertures extending to  $>10$  arcseconds could be used for photometry, much larger than the radius where the effective flux from the star asymptotes to an “infinite” value. For reference, the enclosed flux within an aperture of radius 2 arcseconds is  $>98\%$  of the total flux at all WFC3/UVIS wavelengths (see Hartig 2009 and Kalirai et al. 2009). In all observations, the star was exposed for an integration time that ensured a high signal-to-noise (i.e.,  $>100$ ) detection. For most wide band filters, this typically implied exposure times of just a few seconds, and so 2 – 4 dithered observations (with dithers of 10’s of pixels) were typically obtained in each filter at each epoch.

We performed all of our analysis on both calwf3 processed `_flt` images and dither combined `_drz` images from multidrizzle. We found that the count rate of our sources in these two data products agree to a small fraction of a percent (see Rajan et al. 2010, in prep). For the remaining analysis, our formal measurements represent photometry from the `_flt` images, corrected by the pixel area map (available at <http://www.stsci.edu/hst/wfc3> – see Kalirai et al. 2010). All individual `_flt` images were also subjected to cosmic ray rejection through the lacos Laplacian edge detection program (see van Dokkum 2001).

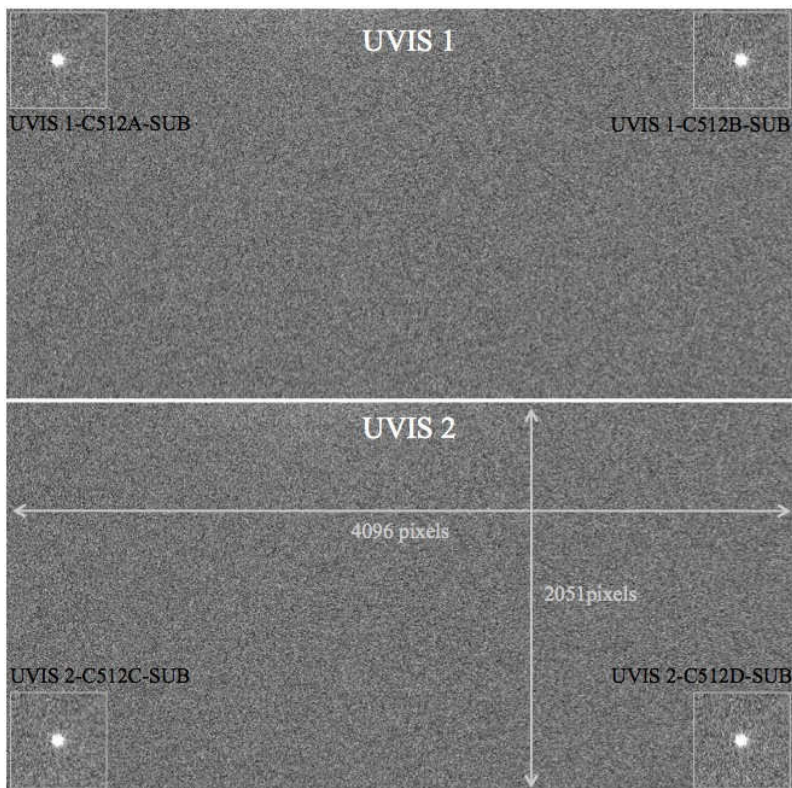


Fig. 1.— The location of the four corner 512 pixel subarrays are shown on the WFC3 mosaic (drawn to scale). Imaging the spectrophotometric standards in these subarrays offers an efficient observing strategy by minimizing readout overheads and buffer dumps. WFC3’s sensitivity provides  $S/N > 100$  detections of these stars in just a few seconds of exposure time in all W band filters.

Aperture photometry of the spectrophotometric standards on all images was performed with the standalone version of DAOPHOT (Stetson 1987; 1994), in a set of 13 apertures with radii ranging from 0.10 to 3.00 arcseconds (2.5 to 75 pixels). The sky was measured as the modal value in an annulus extending from 3.0 to 5.0 arcseconds. An independent analysis with a subset of this data set using the dithered images to remove cosmic rays, and with photometry in IRAF, is in excellent agreement with our results, as discussed in Kalirai et al. (2009). Our final matrix of measurements contains about 30,000 entries, from over 2500 individual observations of the three standards.

Several of the initial observations of G191B2B were obtained with exposure times of 0.5 seconds, and it was quickly discovered that the flux of the star in these data is systematically lower than expected. The same trend was also seen in a very limited number of GD 153 data with 0.5 second exposure times. The WFC3 shutter operates differently for 0.5 second exposures as compared to longer exposures, since the shutter moves continuously through a cycle as opposed to physically stopping and starting. By comparing measurements at 0.5 seconds with longer exposures in the same filters, we’ve calibrated the 0.5 second exposures as actually being 0.486 seconds. This 3%

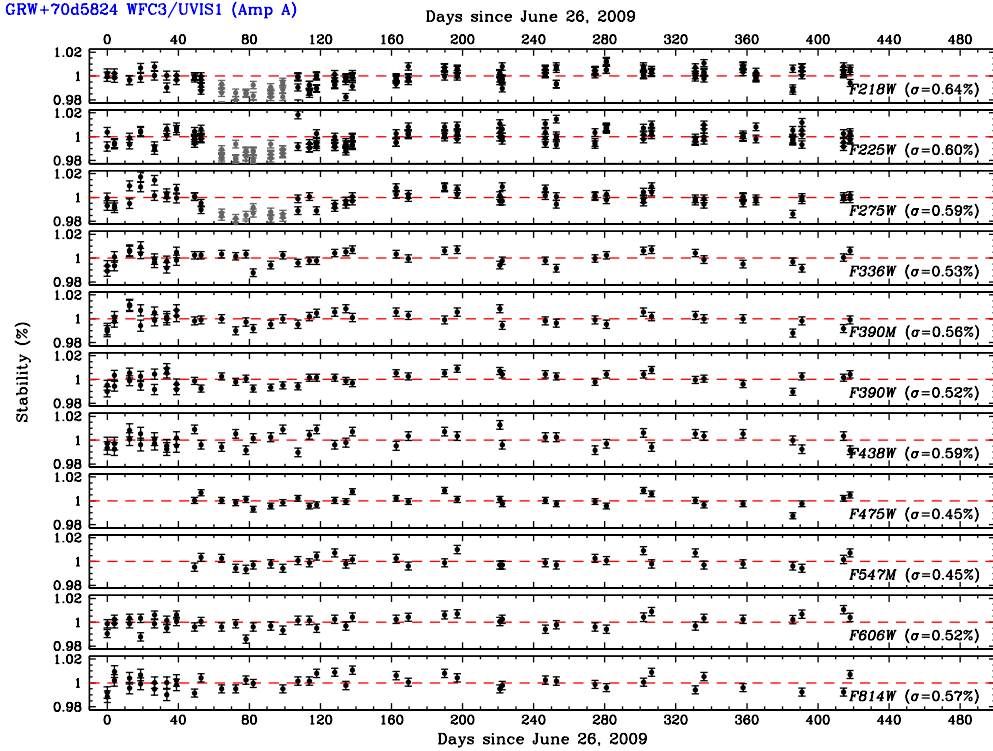


Fig. 2.— Each of the 11 panels illustrates photometric stability measurements for a different WFC3/UVIS filter for the bright standard GRW+70d5824, placed on the UVIS1-C512A-SUB subarray in the corner of UVIS1. All of the individual photometry measurements are shown with  $1\sigma$  photometric errors ( $\sim 0.4\%$ ), relative to the mean brightness over the entire time baseline which stretches from SMOV in June 2009 to August 2010. The large tick marks in each panel represent a 2% variation. Our observations of this star have the best cadence and demonstrate that temporal variations in WFC3/UVIS are  $< 0.4 - 0.6\%$  over the full wavelength range of the detector. As discussed in Section 4, observations in the three UV filters F218W, F225W, and F275W taken shortly after SMOV (days 60 – 100) suffer from a small scale feature in the flat field and so we ignore those data (grey points). If we include these data, the standard deviation in these three filters increases from  $\sigma = 0.6\%$  to  $0.9\%$ . This feature is not present in the Amp C images (see Figure 3).

difference appears to be repeatable with a small scatter ( $\sigma = 0.003$ ), and so the exposure time reported in the headers of all WFC3 0.5 s exposures has now been adjusted. Previous analysis in Thermal Vacuum and in SMOV also saw similar trends, as described in Hilbert (2009).

#### 4. Measuring WFC3/UVIS’s Temporal Stability

The temporal stability of WFC3 can be characterized from the multiple data sets summarized in Table 1, which span a time baseline from mid June 2009 to August 2010 (14 months). Although

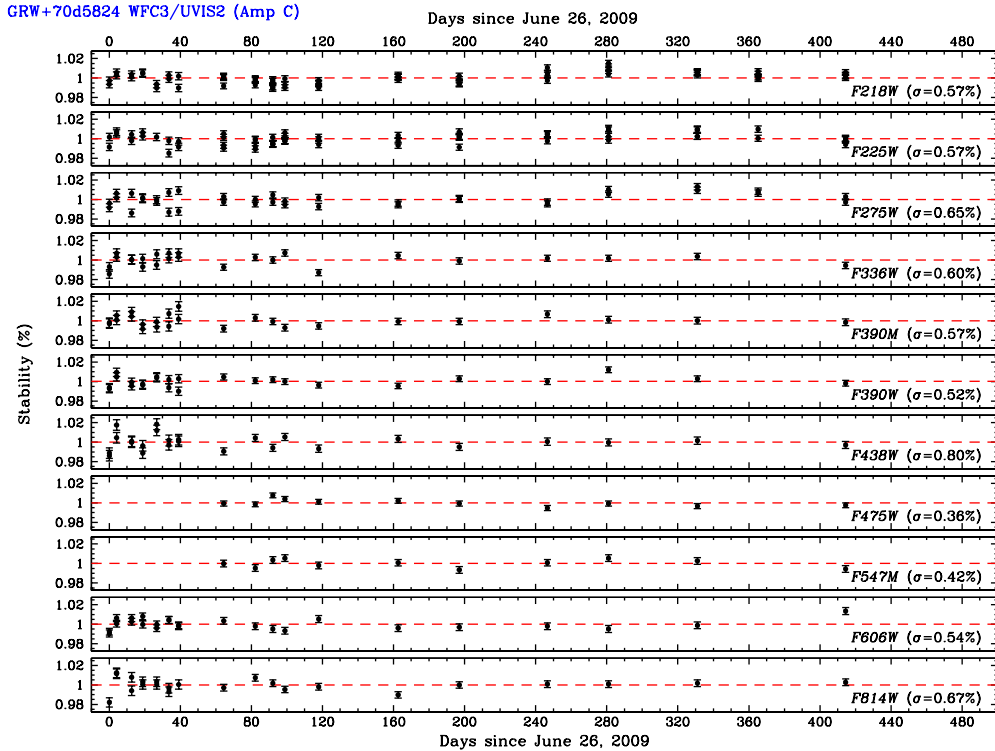


Fig. 3.— Same as Figure 2 for GRW+70d5824, but with the target placed on UVIS2-C512C-SUB.

the observations of GD 153 and G191B2B have different primary goals from the present analysis, the design of these observations provides an excellent data set for stability measurements. For example, given its visibility, GD 153 was observed almost continuously over the first year except during a short  $\sim 3$  month period following SMOV (during which time we observed G191B2B). All of these observations include imaging through most of the widely used WFC3/UVIS filters and also include observations on both detectors. GRW+70d5824 is a secondary HST standard which was observed for the primary purpose of contamination monitoring in the UV filters (as well as F606W and F814W). These observations have a much better cadence than for GD 153 and G191B2B, but have lower signal-to-noise with peak counts in the brightest pixel reaching  $\sim 10,000$  electrons, compared to  $\sim 60,000$  for the primary white dwarf standards.

We illustrate the temporal stability of WFC3 by first treating each of these three stars independently, and further splitting the data set by filter and location on the detector. We define the mean brightness of each star in this configuration over all dither positions and epochs and illustrate the scatter in Figures 2 – 9. All of the measurements shown here reflect photometry in a 0.4 arc-second (i.e., 10 pixel) radius aperture, although we have verified that similar results are obtained for other apertures. First, we present the analysis for the observations with the best cadence and spatial coverage, GRW+70d5824. This star was observed on all four subarrays as shown in Figure 2 (UVIS1-C512A-SUB), Figure 3 (UVIS2-C512C-SUB), Figure 4 (UVIS1-C512B-SUB), and Figure 5

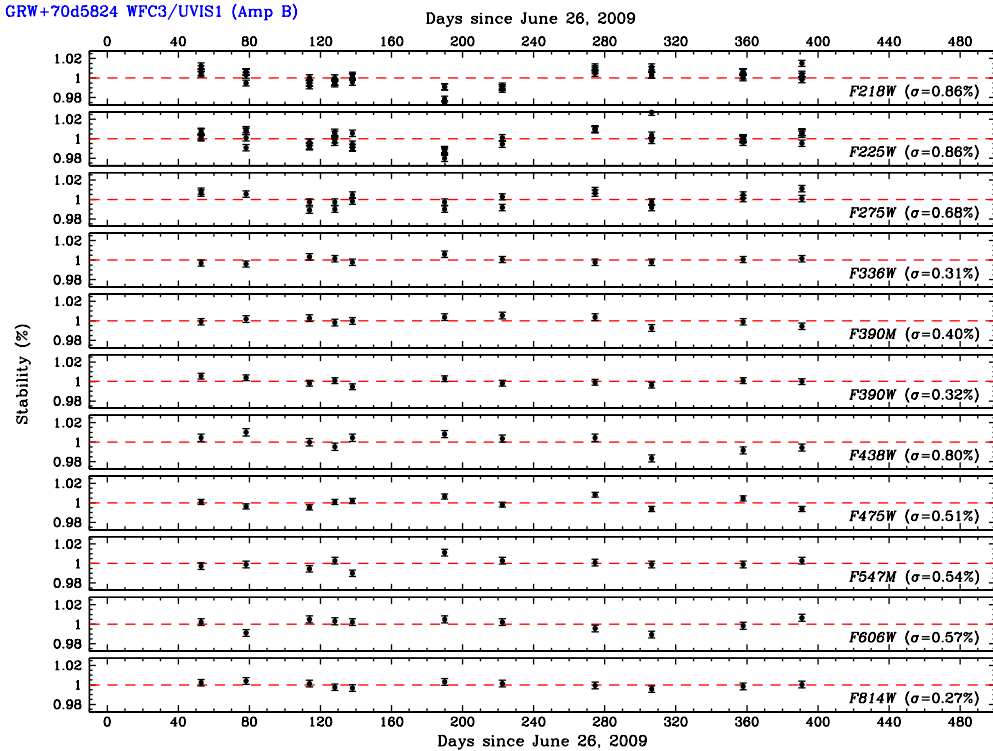


Fig. 4.— Same as Figure 2 for GRW+70d5824, but with the target placed on UVIS1-C512B-SUB.

(UVIS2-C512D-SUB). Of the 18 filters, 11 were observed consistently for several months following SMOV and so we concentrate on these. Most of the observations for this star were either single exposures or two dithered exposures, and so we illustrate all individual measurements as made on `_flt` files. In each of the panels, the large tick marks indicate a  $\pm 2\%$  variation and almost all data points fall within these bounds. The photometric uncertainties in each of the individual measurements is  $\sim 0.4\%$  for these data, as shown by the error bars. Formally, the measured standard deviation in these temporal WFC3/UVIS measurements ranges from 0.3 – 0.6%, from F218W in the UV to F814W in the optical. These data therefore demonstrate that WFC3/UVIS is temporally stable to  $\sim 99.5\%$  over its first year of science operations. For the observations taken solely after SMOV in Figure 4 and 5, the standard deviations in many of the optical filters are  $< 0.4\%$ .

Our analysis of GRW+70d5824 excludes a subset of the data set which was taken in three UV filters on UVIS1-C512A-SUB, between the dates of August 25th and October 4th 2010. These observations, shortly after SMOV concluded, are affected by small scale residual variations in the ground flat of F218W, F225W, and F275W, and are shown in Figure 2 as grey data points that fall well below the mean. Future new on-orbit flats should remove the spatial variations that are affecting the photometry of the star. The features are not present in the Amp C images.

In Figures 6 and 7 we illustrate similar plots of WFC3’s temporal stability as measured using

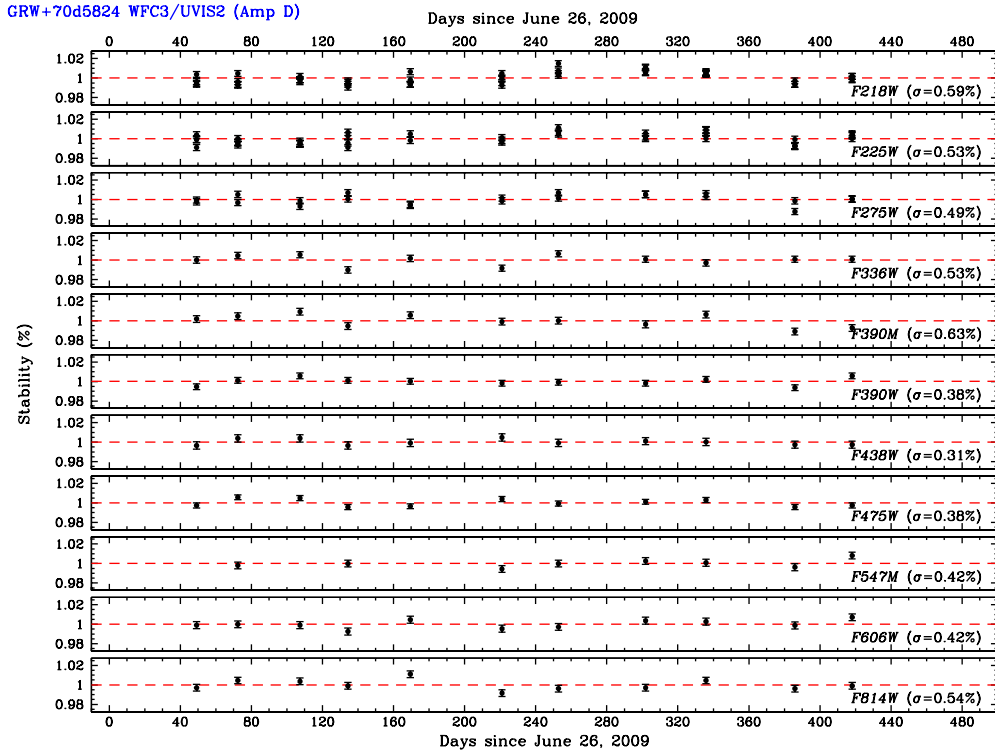


Fig. 5.— Same as Figure 2 for GRW+70d5824, but with the target placed on UVIS2-C512D-SUB.

the bright HST spectrophotometric standard GD 153 (UVIS1-C512A-SUB and UVIS2-C512C-SUB). Our observations of this star consisted of four point dithers at each epoch and so we have averaged the photometry to illustrate a single data point at each date. The scale of these plots is twice as compact as for GRW+70d5824, with each of the big tick marks now representing just 1% variations. The errors bar on each of the data points reflect the standard error in the mean of the four dithered positions, and is typically  $<0.2\%$ . These higher signal-to-noise data sets illustrate that WFC3 is temporally stable to  $<0.5\%$  in all observed filters, which includes W, M, and N bands. The best data sets are for optical W band filters on UVIS1, where the standard deviations are  $\sim 0.3\%$ . For UVIS2 (i.e., Figure 7), we have only four epochs and so we do not quote a formal standard deviation although the four data points show very little scatter.

Finally, we illustrate similar measurements for G191B2B in Figures 8 and 9. This star has the poorest cadence for stability measurements and some of the standard deviations are therefore poorly constrained. However, the data still confirm that WFC3 is temporally stable to the accuracy of the data.



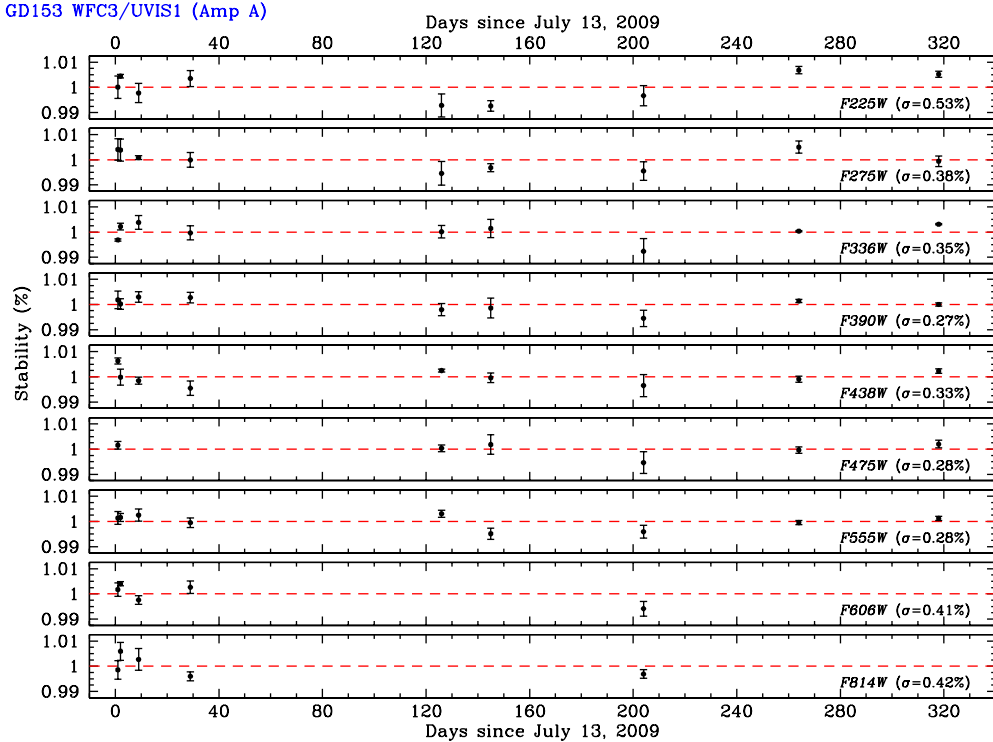


Fig. 6.— The temporal stability of WFC3/UVIS as measured from higher signal-to-noise observations of the bright HST spectrophotometric standard GD 153 on UVIS1-C512A-SUB. At each of the epochs, four dither positions were obtained and averaged together, where the error bars reflect the  $1\sigma$  error in the mean. Relative to Figures 2–5, the vertical scale of each of the individual panels shown here is a factor of two tighter, with large tick marks representing 1% variations. All but a single W band filter (F218W –  $\sigma = 0.5\%$ ) shown here have standard deviations of  $<0.4\%$ . Note that observations of F606W and F814W in the bottom two panels were intentionally shifted to UVIS2 (see Figure 7) at certain epochs (as indicated in Table 1).

## 5. Conclusions

We have analyzed  $\sim 2500$  individual observations of bright HST spectrophotometric standards to establish the temporal stability of WFC3/UVIS over its first year of science operations. All of the observations analyzed in this ISR were taken with the star placed on a small 512 pixel subarray at one of the four corners of the detector. Our analysis indicates that WFC3/UVIS is temporally stable to a high degree. For GRW+70d5824, our measurements on all four corners of the full WFC3 mosaic indicate that temporal variations are only 0.3 – 0.6%, approximately the level of the errors on the measurements. For higher signal-to-noise measurements of GD 153 and G191B2B, the standard deviations in most W band filters are lower (i.e.,  $<0.4\%$ ).

Throughout Cycle 18, we will continue a monitoring campaign to expand the time baseline

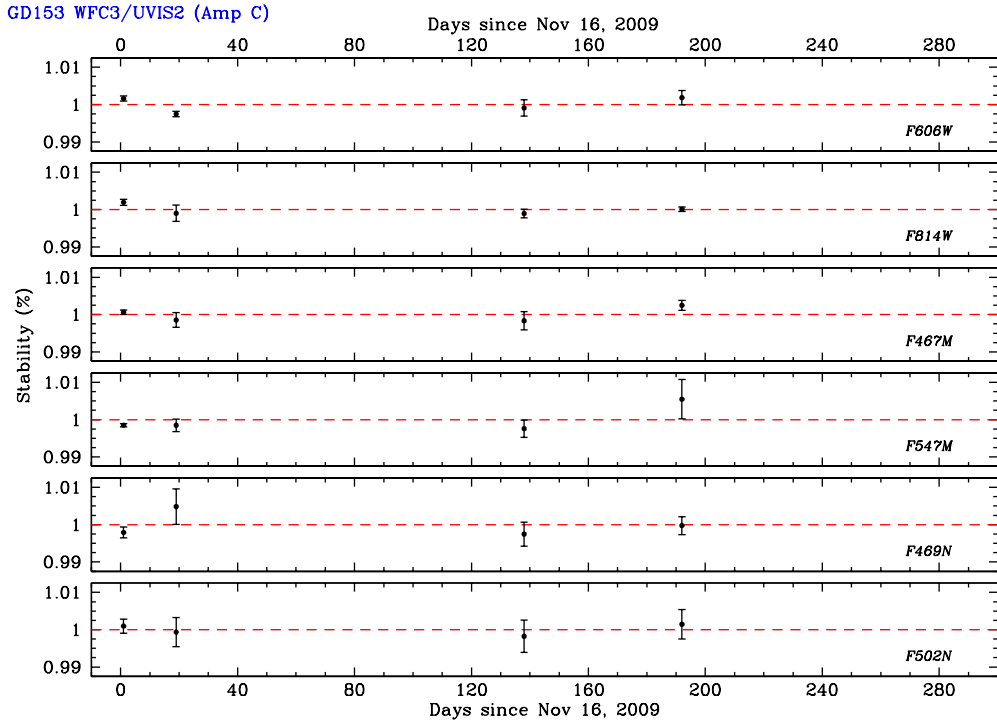


Fig. 7.— Same as Figure 6 for GD 153, but with the target placed on UVIS2-C512C-SUB. Given the limited number of epochs observed thus far, we do not quote formal standard deviations in these measurements. However the four data points for each filter show minimal variations relative to the mean.

over which WFC3’s stability is measured. These new observations will be taken in a subset of filters with higher signal-to-noise to drive the uncertainty in temporal stability measurements to a very low level.

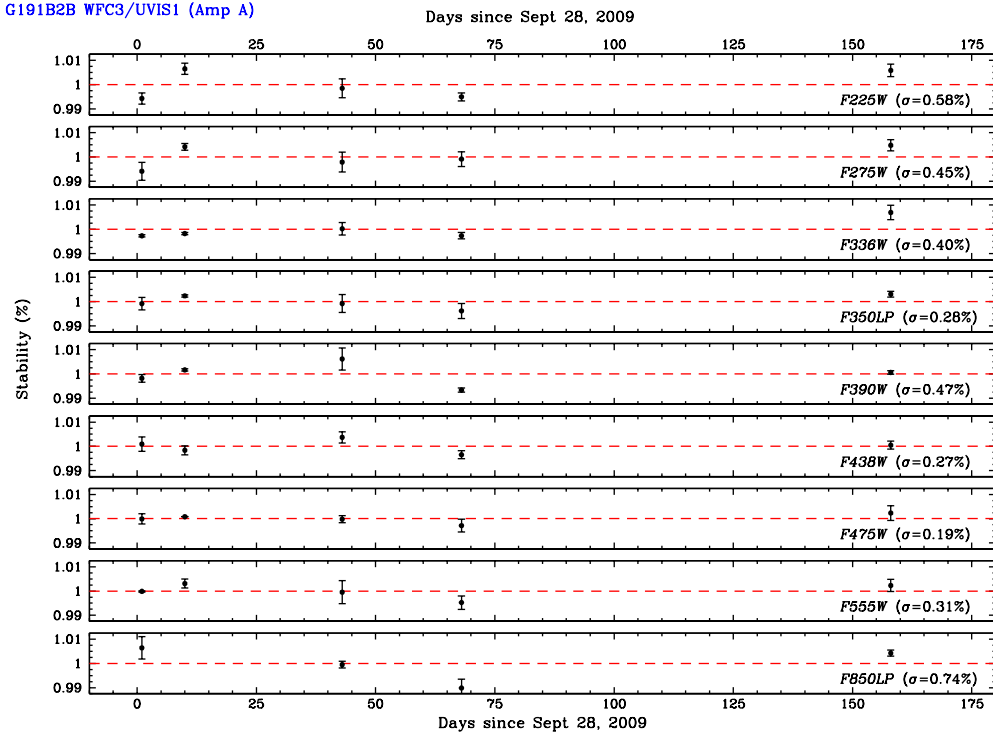


Fig. 8.— The temporal stability of WFC3/UVIS as measured from higher signal-to-noise observations of the bright HST spectrophotometric standard G191B2B on UVIS1-C512A-SUB. The features of this plot are identical to Figure 6 for GD 153, where large tick marks indicate 1% variations and error bars reflect errors in the mean from averaged measurements at each epoch. The measured standard deviations in these observations are very similar to our GD 153 data, with most filters exhibiting a scatter that is  $<0.4\%$ .

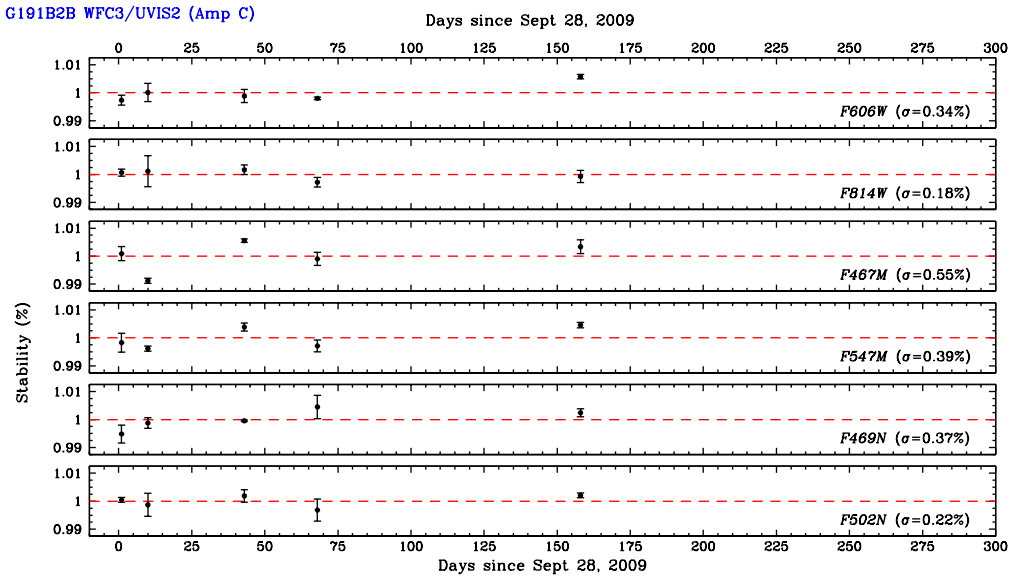


Fig. 9.— Same as Figure 8 for G191B2B, but with the target placed on UVIS2-C512C-SUB.

## References

- Hartig, G. 2009, WFC3 ISR 2009-38 (CAL11436 and CAL11438), “WFC3 SMOV Programs 11436/8: UVIS On-Orbit PSF Evaluation”
- Hilbert, B. 2009, WFC3 ISR 2009-25, “UVIS Channel Shutter Shading”
- Kalirai, J., et al. 2009, WFC3 ISR 2009-31 (CAL11450), “WFC3 SMOV Proposal 11450: The Photometric Performance and Calibration of WFC3/UVIS”
- Kalirai, J., et al. 2010, WFC3 ISR 2010-08, “WFC3 Pixel Area Maps”
- Sabbi, E., 2009, WFC3 ISR 2009-19 (CAL11452), “WFC3 SMOV Program 11452: UVIS Flat Field Uniformity”
- Stetson, P. B. 1987, PASP, 99, 191
- Stetson, P. B. 1994, PASP, 106, 250
- van Dokkum, P. G. 2001, PASP, 113, 1420